

University of Nebraska - Lincoln

DigitalCommons@University of Nebraska - Lincoln

Christian Binek Publications

Research Papers in Physics and Astronomy

10-30-2007

Isothermal low-field tuning of exchange bias in epitaxial Fe/ Cr₂O₃/Fe

Sarbeswar Sahoo

University of Nebraska-Lincoln, sarbeswar@gmail.com

Tathagata Mukherjee

University of Nebraska-Lincoln, tatha.muk@gmail.com

Kirill D. Belashchenko

University of Nebraska-Lincoln, belashchenko@unl.edu

Christian Binek

University of Nebraska-Lincoln, cbinek@unl.edu

Follow this and additional works at: <https://digitalcommons.unl.edu/physicsbinek>



Part of the [Physics Commons](#)

Sahoo, Sarbeswar; Mukherjee, Tathagata; Belashchenko, Kirill D.; and Binek, Christian, "Isothermal low-field tuning of exchange bias in epitaxial Fe/Cr₂O₃/Fe" (2007). *Christian Binek Publications*. 33. <https://digitalcommons.unl.edu/physicsbinek/33>

This Article is brought to you for free and open access by the Research Papers in Physics and Astronomy at DigitalCommons@University of Nebraska - Lincoln. It has been accepted for inclusion in Christian Binek Publications by an authorized administrator of DigitalCommons@University of Nebraska - Lincoln.

Isothermal low-field tuning of exchange bias in epitaxial Fe/Cr₂O₃/Fe

S. Sahoo, T. Mukherjee, K. D. Belashchenko, and Ch. Binék^{a)}

Department of Physics and Astronomy and the Nebraska Center for Materials and Nanoscience, University of Nebraska, Lincoln, Nebraska 68588-0111, USA

(Received 13 August 2007; accepted 2 October 2007; published online 23 October 2007)

Moderate dc magnetic fields of less than 1 T allow tuning the exchange bias in an epitaxially grown Fe 10 nm/Cr₂O₃ 2.7 nm/Fe 10 nm trilayer between negative and positive bias fields. Remarkably, this tunable exchange bias is observed at least up to 395 K which exceeds the Néel temperature of bulk Cr₂O₃ (307 K). The presence of spontaneous exchange bias and the absence of training effects at room temperature suggest the existence of stable interface moments independent of antiferromagnetic long range order in Cr₂O₃. Furthermore, the coercivity remains constant, independent of the exchange bias field. In contrast, large training associated with nonequilibrium spin configurations of antiferromagnetically ordered Cr₂O₃ appears below 50 K. © 2007 American Institute of Physics. [DOI: 10.1063/1.2801519]

The majority of today's realized spintronic devices¹⁻³ utilize the exchange bias⁴ (EB) effect.⁵⁻⁸ The latter is a fundamental proximity effect taking place at the interfaces of magnetic heterostructures including ferromagnetic (F)/antiferromagnetic (AF), F/ferrimagnetic, soft F/hard F systems, and others. Conventionally, EB is established by field cooling the heterostructure below the Néel temperature T_N , or by applying a magnetic field during the fabrication process. EB manifests itself in the shift of the hysteresis loop along the magnetic field axis and a concomitant increase in the coercivity $\mu_0 H_c$. The EB magnitude $\mu_0 H_{eb}$ depends on intrinsic parameters such as the exchange coupling at the F/AF interface, interface roughness, individual F and AF micro(magnetic) structure, or their thicknesses. However, it has been reported that EB can be tuned by various extrinsic parameters. In this context, a broad spectrum of experimental protocols has been employed: cooling in different magnetic fields,⁹ cooling in zero field from different magnetization states,¹⁰ cooling in combinations of dc and ac fields,¹¹ or saturating the F in large negative fields and then measuring the remaining loop with different waiting times.^{12,13} Other irreversible approaches such as high-temperature annealing¹⁴ or ion irradiation¹⁵ have also been used. Nogués *et al.*,¹⁶ reported that EB can be tuned at room temperature by subjecting the system to pulsed fields as high as 55.6 T. All these attempts to tune EB externally involve tedious experimental treatments or impractically large magnetic fields not easily available, which make them unsuitable for practical applications.

In this letter, we present an epitaxially grown Fe 10 nm/Cr₂O₃ 2.7 nm/Fe 10 nm trilayer structure and demonstrate that EB can be tuned at room temperature by subjecting the system to moderate dc magnetic fields, $-1 \leq \mu_0 H_{dc} \leq 1$ T. The motivation of using Cr₂O₃ as the AF layer is based on our recent observation of an appreciable moment in single Cr₂O₃ films.¹⁷ There the direction of the induced moment could be controlled by an applied dc field. Coupling of a tunable pinning moment to an adjacent F film is anticipated to provide tunable EB.

Moreover, EB above T_N of the AF has recently been observed in other F-AF systems such as Co/NiF₂ (Ref. 18),

Fe₃O₄/CoO (Ref. 19), and Ni₈₀Fe₂₀/Co₃O₄ (Ref. 20). There it is primarily attributed to either strain or proximity effects at the F/AF interfaces. In our trilayer, the EB is stable up to the highest measured temperature $T=395$ K, which is far above the bulk Néel temperature of Cr₂O₃, $T_N=307$ K. Here, we explore the possibility of using dc fields to control the EB effect. Unlike previous studies, our system does not require any specific field-cooling procedure.

The trilayer system, Fe 10 nm/Cr₂O₃ 2.7 nm/Fe 10 nm, is prepared in a molecular beam epitaxy chamber at a base pressure of 1×10^{-10} mbar. The (0001)-oriented *c*-Al₂O₃ substrate is heated to and maintained at 573 K during the deposition process. Note that no external magnetic field was present during the deposition. A stoichiometric Cr₂O₃ film was grown by thermal evaporation of Cr metal in an O₂ partial pressure of 2.2×10^{-6} mbar.¹⁸ Growth rates of Fe and Cr₂O₃ were 0.37 and 0.28 nm/min.

Analysis of the large-angle x-ray diffraction pattern (Max-B, Rigaku D) in Fig. 1 illustrates that single-crystalline Fe and Cr₂O₃ films are formed. The (110)-oriented bcc Fe peak shows pronounced Laue oscillations originating from coherently scattering Fe (110) lattice planes. The distribution of scattered intensity around the central maximum at $2\theta = 44.67^\circ$ is fitted by the one-dimensional Laue diffraction function

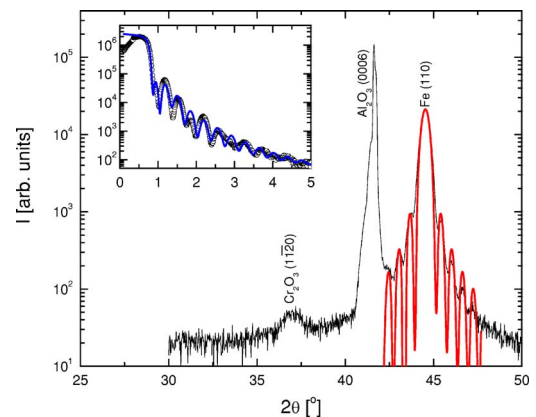


FIG. 1. (Color online) X-ray diffraction pattern of Fe 10 nm/Cr₂O₃ 2.7 nm/Fe 10 nm trilayer. Solid lines are the fit to the Laue function according to Eq. (1). The inset shows small angle x-ray reflection data (circles) and the best fit (line) by using LEPTOS-2 program.

^{a)}Electronic mail: cbinék2@unl.edu

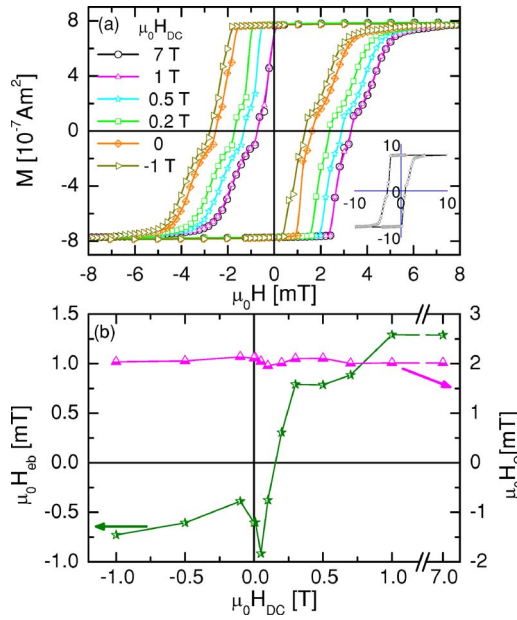


FIG. 2. (Color online) (a) Representative hysteresis loops at $T=300$ K after subjecting the trilayer to various dc fields. The inset shows a loop at $T=395$ K and $\mu_0 H_{dc}=0$. (b) $\mu_0 H_{eb}$ and $\mu_0 H_c$ vs $\mu_0 H_{dc}$. Lines are guide to the eye.

$$L = L_0 \frac{\sin^2(NKd/2)}{\sin^2(Kd/2)}, \quad (1)$$

where N is the number of coherently scattering planes, d is the spacing between the Fe (110) planes, $K=2k_0 \sin 2\theta$ with θ being the scattering angle, $k_0=2\pi/\lambda$ the magnitude of wave vector and $\lambda_{Cu K\alpha}=0.154$ nm the wavelength of the x-ray source. Best fit of the experimental data to Eq. (1) with fixed $\lambda=0.154$ nm yields $N=79\pm 0.02$ and $d=0.204\pm 0.001$ nm. The value of d is in close agreement with the bulk $d_{110}=0.203$ nm. This infers that the Fe film thickness contributing to the coherent scattering is $Nd=16$ nm. The high texture quality of the films was furthermore corroborated by small values $\omega < 0.04^\circ$ of the full width at half maximum observed in the rocking curve scan performed around Fe (110) peak. Analysis of the Cr_2O_3 film peak reveals (11 $\bar{2}$ 0)-textured growth. The inset of Fig. 1 shows the small angle x-ray reflectivity (SAXR) diagram (AXS-D8 Discover, Bruker) of the trilayer structure. Fit of these data by using LEPTOS-2 software indicates a Fe 10 ± 0.4 nm/ Cr_2O_3 2.72 ± 0.18 nm/Fe 10.8 ± 0.3 nm trilayer structure, which is in excellent agreement with the desired system.

The magnetic measurements were carried out using the superconducting quantum interference device (SQUID) magnetometer (MPMS-XL, Quantum Design) with fields applied in the sample plane. Figure 2(a) shows hysteresis loops measured at $T=300$ K after subjecting the system to zero or finite dc fields. The exchange biased hysteresis loops have remanent to saturation magnetization ratio $M_r/M_s=1$. They also exhibit asymmetry with respect to the coercive fields in the respective up and down branches. It may originate from the small difference in $\mu_0 H_c$ values of the top and bottom Fe layers resembling the scenario of a thick-thin layer switching process.²¹

Remarkably, Fig. 2(a) shows that nonzero EB is present for zero $\mu_0 H_{dc}$. This spontaneous EB is observed in the virgin sample after preparation at 573 K without any magnetic field treatment which could have magnetized the Fe films.

The hysteresis loop shift (EB) always means that the magnetic structure of the system has a reversible component that lifts the degeneracy of the state magnetized in the opposite direction. In our case, EB free from any training effect persists well above bulk T_N of Cr_2O_3 , and therefore, barring large proximity effects, it appears unlikely that the EB originates from exchange coupling with the antiferromagnet. It may be explained by the presence of magnetically hard regions that are only reversed by strong dc fields. Such regions may appear, for example, due to the formation of chemically modified interface regions such as Fe_3O_4 with high Curie temperatures. The presence of magnetically hard regions reaching even into the F film is consistent with recent neutron reflectometry studies.²²

We find that the sign of $\mu_0 H_{eb}$ can be controlled exclusively by $\mu_0 H_{dc}$ in our trilayer. This is reminiscent of the scenario of changing the sign of $\mu_0 H_{eb}$ depending on the strength of the cooling fields.⁹ Note, however, that our EB tuning takes place *isothermally* where the pinning magnetization is reversed by a magnetic field only without breaking and reestablishing AF long range order during a field cooling process. Competition between AF exchange coupling of the pinning and the Fe magnetizations with the Zeeman interaction energy of the pinning system determines the sign of $\mu_0 H_{eb}$. For $\mu_0 H_{dc} \leq 0.2$ T, AF coupling remains dominant over the Zeeman energy, resulting in regular (negative) EB. For larger $\mu_0 H_{dc}$, the Zeeman interaction overcomes the AF exchange coupling which aligns the pinning moments parallel to larger $\mu_0 H_{dc}$, leading to positive EB. Note that recently Cheon *et al.* pointed out that EB fields can be reversed in all EB systems below the blocking temperature via reversal of the uncompensated pinning magnetization.²³ However, the isothermal field tuning described here takes place at easily accessible magnetic fields of less than 1 T, and does not depend on long range AF order.

Figure 2(b) shows $\mu_0 H_{eb} = \mu_0(H_+ + H_-)/2$ and $\mu_0 H_c = \mu_0(H_+ - H_-)/2$ vs $\mu_0 H_{dc}$, where $\mu_0 H_+$ and $\mu_0 H_-$ are the field values at which the magnetization becomes zero on right and left branch of the hysteresis loop, respectively. While $\mu_0 H_c$ remains unchanged to within 1% of its mean value of ~ 2 mT, $\mu_0 H_{eb}$ varies in the range $-0.9 \leq \mu_0 H_{eb} \leq 1.2$ mT depending on the dc field. Note that identical EB fields have been determined from alternating gradient force magnetometry using electromagnets to generate the dc fields. Hence, trapped flux in the superconducting coils of the SQUID magnetometer is unambiguously excluded. It is also important to mention that the results are independent of the duration the system is subjected to the dc field. Indeed, we measured the same hysteresis loops with exposure times of 10, 100, and 300 s. The results presented in this letter correspond to exposure duration of 100 s.

Training of the exchange bias effect offers a unique tool to test the deviation from the equilibrium of the AF layer.²⁴ To this end, we measured the training effect after tuning the exchange bias by various dc fields. Shown in Fig. 3(a) are the results at 300 K with $\mu_0 H_{dc}=1$ and -1 T, respectively. Note that these loop shifts resemble positive EB. Clearly, the hysteresis loops remain unchanged implying the absence of any aging phenomena and, hence, indicating that this unusual high temperature exchange bias phenomenon originates from a stable interface moment. The latter is independent of the AF long range order which establishes at lower temperatures.

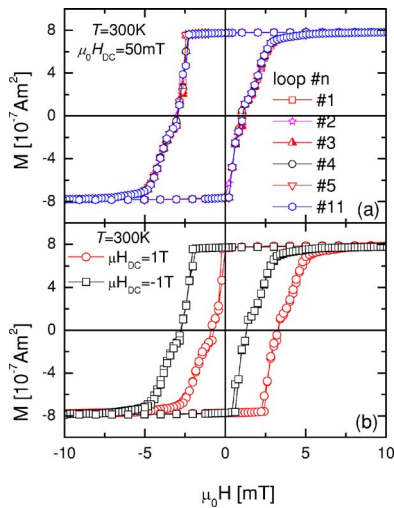


FIG. 3. (Color online) (a) Room temperature training cycles after subjecting the trilayer to $\mu_0 H_{dc} = 50$ mT indicating the absence of any training effect. (b) Two consecutive loops measured after subjecting the trilayer to $\mu_0 H_{dc} = 1$ T (circles) and -1 T (squares), respectively.

In contrast to the results at 300 K, EB measured at 10 K reveals huge training effects associated with the nonequilibrium AF configuration of the Cr_2O_3 film below $T^* \approx 50$ K, which leaves its fingerprints in the $M/\mu_0 H$ vs T curve [inset of Fig. 4(a)] measured at a field of 10 mT. Figure 4(a) presents selected hysteresis loops at 10 K within a training sequence after field cooling from 395 K in a field of 50 mT. The gradual decrease of $\mu_0 H_{eb}$ (open squares) and $\mu_0 H_c$ (circles) with the subsequent loop number n plotted in Fig. 4(b) shows the usual training behavior, indicating AF long range order and its spin configurational relaxation. This aging process continues until the AF reaches its quasiequilibrium state in the limit $n \rightarrow \infty$. The solid squares repre-

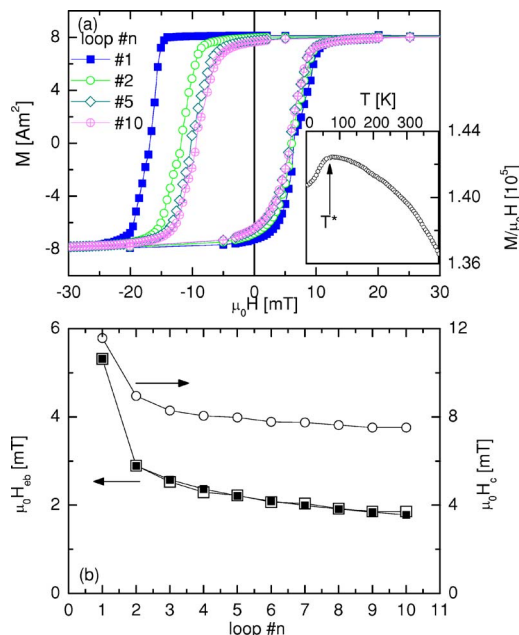


FIG. 4. (Color online) (a) Regular training effect at $T = 10$ K after field cooled from $T = 395$ K in $\mu_0 H = 50$ mT. The inset shows $M/\mu_0 H$ vs T measured at $\mu_0 H = 10$ mT. (b) $\mu_0 H_{eb}$ (open squares) and $\mu_0 H_c$ (circles) vs loop number, n . The solid symbols are the best fit of Eq. (2) to the training data. Lines are guide to the eye.

sent the best fit of $\mu_0 H_{eb}$ vs n data to a recently developed phenomenological theory,²⁴

$$\mu_0 [H_{eb}(n+1) - H_{eb}(n)] = -\gamma [\mu_0 (H_{eb}(n) - H_{eb}^c)]^3, \quad (2)$$

where $\gamma = 2 \times 10^{-4} (\text{mT})^{-2}$ and $\mu_0 H_{eb}^c = 0.4$ mT were obtained as the two fitting parameters. γ contains the interface exchange coupling and the damping constant governing the relaxation dynamics of the AF spin configuration while $\mu_0 H_{eb}^c$ is the quasiequilibrium exchange bias field.²⁴

In conclusion, we found that exchange bias resulting from pinned interface magnetization in an epitaxial $\text{Fe}/\text{Cr}_2\text{O}_3/\text{Fe}$ trilayer is isothermally tunable by moderate dc magnetic fields at room temperature. This behavior is distinct from regular exchange bias in the sense that it does not rely on field-cooling treatments and shows no training effect. It indicates that the pinning magnetization is independent of the long range AF order in the Cr_2O_3 spacer. Regular exchange bias with pronounced training behavior is, however, recovered below 50 K. Isothermally tunable exchange bias with moderate fields at room temperature is expected to impact future spintronic devices.

This work was supported by NRI, NCSER, NSF through Career DMR-0547887 and NSF MRSEC DMR-0213808.

¹G. A. Prinz, *Science* **282**, 1660 (1998).

²S. S. P. Parkin, K. P. Roche, M. G. Samant, P. M. Rice, R. B. Beyers, R. E. Scheuerlein, E. J. O'Sullivan, S. L. Brown, J. Bucchigano, D. W. Abraham, Y. Lu, M. Rooks, P. L. Trouilloud, R. A. Wanner, and W. J. Gallagher, *J. Appl. Phys.* **85**, 5828 (1999).

³S. A. Wolf, *Science* **294**, 1488 (2001).

⁴W. H. Meiklejohn and C. P. Bean, *Phys. Rev.* **105**, 904 (1957).

⁵J. Nogués and I. K. Schuller, *J. Magn. Magn. Mater.* **192**, 203 (1999).

⁶A. Berkowitz and K. Takano, *J. Magn. Magn. Mater.* **200**, 552 (1999).

⁷R. L. Stamps, *J. Phys. D* **33**, R247 (2000).

⁸M. Kiwi, *J. Magn. Magn. Mater.* **234**, 584 (2001).

⁹J. Nogués, D. Lederman, T. J. Moran, and I. K. Schuller, *Phys. Rev. Lett.* **76**, 4624 (1996).

¹⁰P. Miltényi, M. Gierlings, M. Bammig, U. May, G. Güntherodt, J. Nogués, M. Gruyters, C. Leighton, and I. K. Schuller, *Appl. Phys. Lett.* **75**, 2304 (1999).

¹¹N. J. Gökemeijer, J. W. Cai, and C. L. Chien, *Phys. Rev. B* **60**, 3033 (1999).

¹²P. A. A. van der Heijden, T. F. M. M. Maas, W. J. M. de Jonge, J. C. S. Kools, F. Roozeboom, and P. J. van der Zaag, *Appl. Phys. Lett.* **72**, 492 (1998).

¹³T. Hughes, K. O'Grady, H. Laidler, and R. W. Chantrell, *J. Magn. Magn. Mater.* **235**, 329 (2001).

¹⁴M. G. Samant, J. A. Lüning, J. Stöhr, and S. S. P. Parkin, *Appl. Phys. Lett.* **76**, 3097 (2000).

¹⁵T. Mewes, R. Lopusnik, J. Fassbender, B. Hillebrands, M. Jung, D. Engel, A. Ehresmann, and H. Schmoranzler, *Appl. Phys. Lett.* **76**, 1057 (2000).

¹⁶J. Nogués, J. Sort, S. Suriñach, J. S. Muñoz, M. D. Baró, J. F. Bobo, U. Lüders, E. Haanappel, M. R. Fitzsimmons, A. Hoffmann, and J. W. Cai, *Appl. Phys. Lett.* **82**, 3044 (2003).

¹⁷S. Sahoo and Ch. Binek, *Philos. Mag. Lett.* **87**, 259 (2007).

¹⁸H. Shi, D. Lederman, K. V. O'Donovan, and J. A. Borchers, *Phys. Rev. B* **69**, 214416 (2004).

¹⁹P. J. Van der Zaag, Y. Ijiri, J. A. Borchers, L. F. Feiner, R. M. Wolf, J. M. Gaines, R. W. Erwin, and M. A. Verheijen, *Phys. Rev. Lett.* **84**, 6102 (2000).

²⁰J. van Lierop, K.-W. Lin, J.-Y. Guo, H. Ouyang, and B. W. Southern, *Phys. Rev. B* **75**, 134409 (2007).

²¹T. Ambrose and C. L. Chien, *Appl. Phys. Lett.* **65**, 1967 (1994).

²²M. R. Fitzsimmons, B. J. Kirby, S. Roy, Z.-P. Li, I. V. Roshchin, S. K. Sinha, and I. K. Schuller, *Phys. Rev. B* **75**, 214412 (2007).

²³M. Cheon, Z. Liu, and D. Lederman, *Appl. Phys. Lett.* **90**, 012511 (2007).

²⁴Ch. Binek, *Phys. Rev. B* **70**, 014421 (2004).